International Research Journal of Multidisciplinary Scope (IRJMS), 2026; 7(1): 799-814

IRJMS

Original Article | ISSN (O): 2582-631X DOI: 10.47857/irjms.2026.v07i01.07489

Biogenic Synthesis of Copper Oxide Nanoparticles using *Anethum graveolens*; Antibacterial, Anticancer and Therapeutic Potential *in vitro* Analysis

Kodiganti Naresh Kumar[1], Tharani Munusamy[1], Malchi Suresh[1], Manju Bhargavi S[2], Nalini Devarajan[1]*

[1]Central Research Laboratory, Meenakshi Academy of Higher Education and Research, Chennai-600078, Tamil Nadu, India, [2]Nutrition & Dietetics, Faculty of humanities and science, Meenakshi Academy of Higher Education and Research, Chennai-600078. Tamil Nadu, India. *Corresponding Author's Email: knareshkumar5173@gmail.com; drnalini.crl@madch.edu.in

Abstract

In this current study, copper-oxide nanoparticles (Cu-ONPs) were produced via an eco-friendly approach with *A. graveolens* (dill) seed aqueous extract as a stabilizing and reducing precursor. This process was revealed by a visible colour transformation from light green to dark green and also confirmed by UV-Vis spectroscopy. Characterization was conducted using techniques that included FTIR, XRD, SEM with EDX, and TEM. UV-Visible spectroscopy revealed broad peaks at 342–380 nm. FTIR spectral analysis revealed the involvement of various functional groups in stabilization. XRD also confirmed the crystallinity of AG-CuONPs, and SEM images showed a predominantly spherical shape with a relatively smooth surface morphology, with agglomeration. TEM images revealed uniformly distributed particles with an average diameter of 45 nm. The AG-CuONPs showed strong anti-bacterial activity against *P. aeruginosa, E. Coli,* and *S. aureus*, with increasing efficacy at higher concentrations. Furthermore, it showed promising antioxidant properties (DPPH assay), anti-inflammatory potential (BSA and EA denaturation tests), and potential anticancer properties against A549 lung cancer cells, with low cytotoxicity toward HEK293 normal cells. These results highlight the potential of dill seed-mediated CuONPs' eco-friendly approach towards the development of novel antimicrobial and anticancer agents. Additional research is required to discover its anticancer activities under an *in vivo* system.

Keywords: *Anethum graveolens*, Antibacterial, Anticancer, Anti-Inflammatory, Antioxidant, Copper Oxide Nanoparticle (CuONPs).

Introduction

Modern research is increasingly turning to natural plant-based therapeutics as alternatives to synthetic drugs due to their side effects and long-term toxicity (1). The growing menace of resistance to antibiotics and anticancer drugs has further boosted interest in this direction (2). Chemotherapy is most commonly used in the treatment of a large variety of cancers. Their use is often limited because of drug resistance, undue toxicity, and organ damage. Due to the resistance and high toxicity, there has been a growing need to explore other, safer forms of therapy (3). According to some research, using plant-based materials in conjunction with nanotechnology for medication delivery would increase treatment effectiveness and reduce harm (4). In recent years, the rapid evolution of the global market in nanomaterials has increased demand in biomedical applications, in diagnostics, drug delivery, anticancer therapy, and treatments of microbial infections (5, 6).

In this context, nanotechnology gained considerable attention due to special physiochemical and biological characteristic properties, especially metal and metal-oxide nanoparticles, have drawn a lot of interest to nanotechnology. Among these, copper-oxide nanoparticles (CuONPs) are significant interest because of their broad-spectrum antibacterial action, affordability, potential anticancer characteristics, biological relevance and low-toxicity (7). However, the conventional method of synthesis of nanoparticles through chemical and physical processes involves dangerous chemicals as well as lots of energy, thus creating health and safety concerns. This rendered such processes ineffective, hence the development of biogenic synthesis, which was an eco-friendly and effective

This is an Open Access article distributed under the terms of the Creative Commons Attribution CC BY license (http://creativecommons.org/licenses/by/4.0/), which permits unrestricted reuse, distribution, and reproduction in any medium, provided the original work is properly cited.

(Received 08th August 2025; Accepted 31st December 2025; Published 22nd January 2026)

way to synthesize nanoparticles using plant extracts (8). The phytochemicals of plants serve as natural stabilizing and reducing agents that minimize toxicity while facilitating controlled nanoparticle formation and green synthesis minimizes chemical wate and energy consumption (9).

Recent research in plant mediated copper oxide nanoparticles revealed enhanced antimicrobial and anticancer properties compared to chemically synthesized. These effects attributed to improved surface area and biological affinity (10). And moreover, CuO nanoparticles known to interact with cellular metabolism by inducing oxidative imbalance, disruption of cellular membrane integrity, and alteration of intracellular signalling pathways, supports the exploration of biologically synthesised CuO nanoparticle in multifunctional therapeutic agent. There are extensive studies on plant-mediated synthesis of copper oxide nanoparticles, the use of *Anethum graveolens* as a biological reducing and stabilizing agent remains largely unexplored.

Dill, or *Anethum graveolens* (*A. graveolens*), is an annual herb used for therapeutic purposes (11). *Anethum*, from the Greek term *aneeton* for strong and distinctive odor, indicative of the plant's typical scent from its essential oils. It belongs to the family of *Apiaceae*, and is indigenous to southeastern Europe, the Mediterranean, and Asia (12). The chief cultivated species of dill are Indian (*A. graveolens*) and European (*Anethum sowa*). The *A. graveolens* essential oil comprises a variety of phytoconstituents, including coumarins, oleic acid, stearic acid, phenolic acids, tannins, flavonoids, palmitic acid, triterpenes, and capric acid. The chief components of total oil composition were limonene, carvone, cis-dihydrocarvone, and trans-carvone, as well as α-phellandrene, dill ether, sabinene, and α-oleic acid (13).

Studies have established that *A. graveolens* possesses various bioactivities, such as anti-inflammatory, anti-diabetic, anti-oxidant, antimicrobic, antispasmodic, and antitumor activities (14, 15). Additionally, its essential oil and seed extracts have demonstrated antimicrobial activity against a range of pathogens, including *Salmonella spp., Bacillus cereus, Enterococcus faecalis, Escherichia coli, Pseudomonas aeruginosa, Mycobacterium spp.,* and *Staphylococcus aureus, Shigella flexneri* (16).

The present study demonstrates an eco-friendly approach to synthesizing CuONPs using aqueous seed extract of *A. graveolens*. An evaluation of their antibacterial activity in *S. aureus, E. coli,* and *P. aeruginosa*. Additionally, anti-oxidant, anti-inflammatory activity, and cytotoxic efficacy towards A549 and HEK293 cell lines.

Materials and Methodology

Materials

All the necessary antibiotics and analytical-grade chemicals required for microbiology assays were obtained from Hi-Media. DPPH (CAS: 1898-66-4) from SRL, Mumbai, India. Dulbecco's Modified Eagle's Medium (DMEM; 11965092, Gibco, ThermoFisher Scientific USA) with high glucose, along with DMEM without phenol-red (Cat; 31053028, Gibco, ThermoFisher Scientific, USA), antibiotics (penicillin-streptomycin, Cat; P4333, Sigma-Aldrich, St. Louis, MO, USA), 0.5% Dissociation reagent (Trypsin-EDTA, Cat; 15400054, Gibco, Grand Island, NY), and Fetal Bovine Serum (FBS, Cat; 26140095, Gibco, Brazil). 3-(4,5-Dimethyl-2-thiazolyl)-2,5-diphenyl-2H-tetrazolium bromide (MTT, Cat; V13154, Invitrogen, Thermo Fisher Scientific, USA). Cell lines HEK293 (Human Embryonic Kidney) and A549 (lung cancer) were procured from NCCS Pune, India.

Methods

Overall experimental workflow employed in this study is summarised in Figure 1.

Collection and Authentication of Seeds: The *A. graveolens* seeds bought from a nearby marketplace, validated by the Central Council for Research in Siddha (CCRS), pharmacognosy specialists (Specimen voucher number: *A. graveolens* L. #A04022506G), Chennai, Tamil Nadu, India.

Preparation of Dill Seed Extracts: The seeds were cleaned with distilled water (DW) and dried in a shed. The dried seeds were powdered using a mortar and pestle. These fine powder specimens were stored in an airtight bottle in a dry place (Figure 2). Aqueous extracts of seeds were prepared by dissolving 1 gram of the above-prepared powder into 100 mL of DW heated at 60º to 70°C for 20 minutes (17). The clear extract was collected through filtration (Whatman No. 1), and this extract was utilized to synthesize copper oxide nanoparticles (AG-CuONPs).

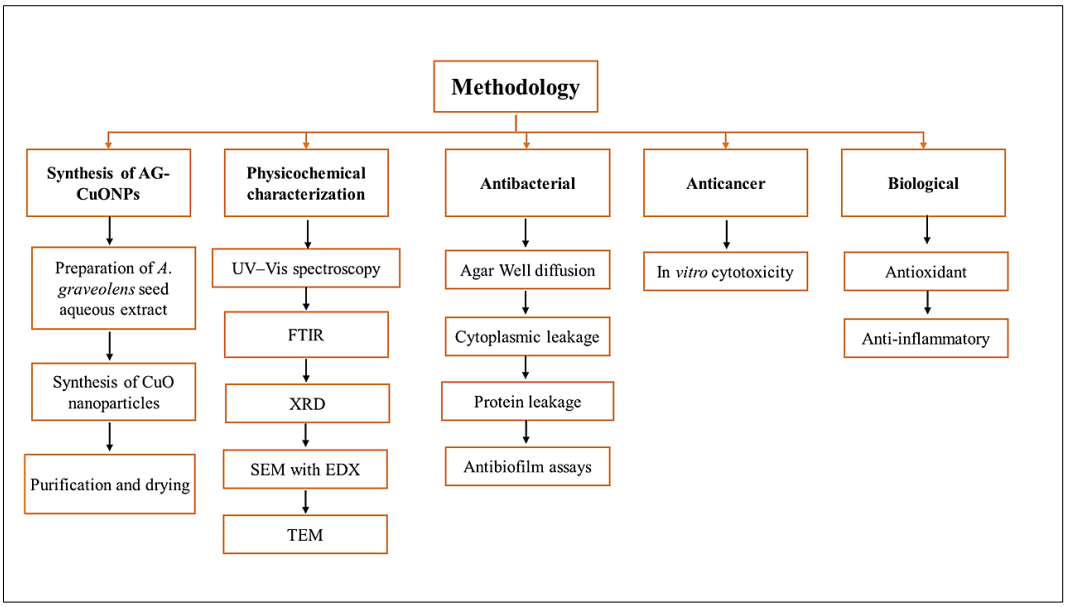

Figure 1: Workflow for the Biogenic Synthesis and Biological Evaluation of AG-CuONPs

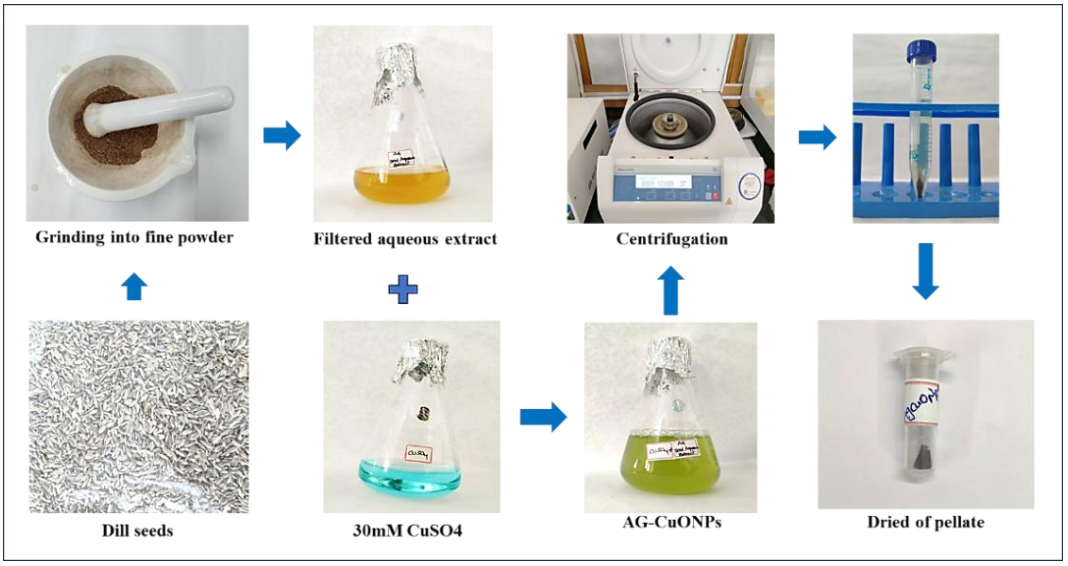

Figure 2: Green Synthesis of Copper Oxide Nanoparticles using *A. graveolens* (AG) Seeds

Preparation of Copper Oxide Nanoparticles (AG-CuONPs): 30 mM copper sulphate ($CuSO_4$) was prepared in 100 mL of DW (Figure 2). 20 mL of extract was mixed with 80 mL of 30 mM $CuSO_4$ solution, and then shifted to a magnetic stirrer for 20 minutes at 800 RPM. Then placed in an orbital shaker at 37ºC with continuous shaking, and observed for any colour change (18). The absorbance was measured from 200 to 700 nm using a UV-Vis spectrophotometer (Shimadzu UV-1900i, Shimadzu CORP, Japan). Synthesised AG-CuONPs was centrifuged at 8000 RPM for 15 minutes, and the pellet was dried under 70°C in a hot air oven, used for further analysis.

Characterization: The UV-Vis spectrometer analysis was used as primary confirmation. Fourier Transform Infrared Spectroscopy (FTIR) analysis was carried out, using an FTIR-1500 spectrophotometer (JOSVOK, China) for functional groups. Crystalline nature was examined by X-ray diffraction (XRD) (BRUKER, Germany), with the incident source of radiation being Kα (λ = 1.54060 Å). Surface morphology was evaluated under Scanning Electron Microscope (SEM) (Carl Zeiss Supra-300, Germany). Energy-Dispersive X-ray (EDX) with a Sigma ZEISS Field Emission was used to validate the elemental composition. The particle size was determined by High-Resolution

Transmission Electron Microscopy (HRTEM) (Talos F200S-G2, Thermo Scientific).

Anti-Oxidant Assay (DPPH): The antioxidative potential of AG-CuONPs was evaluated using the DPPH reagent reported earlier, with minor modifications (19, 20). 4 mL of 0.3 mM DPPH (prepared in MeOH) reagent was mixed with 1 mL of AG-CuONPs (10, 20, 30, 40, and 50µg/mL) and ascorbic acid (standard), which were prepared in methanol. The combination was left in the dark at 30°C for 30 minutes after vigorous shaking. Absorbance O.D. was measured at 517 nm against methanol. The decreased absorbance indicated an increased percentage of free radical scavenging activity, using equation [1].

$$\text{Radical scavenging activity (\%)} = \left(\frac{Abs\ of\ Control - Abs\ of\ Sample}{Abs\ of\ Control}\right) \times 100 \qquad [1]$$

Where, Abs = Absorbance or Optical Density (O.D.); control = with methanol (MeOH); sample = on addition of AG-CuONPS or standard

Anti-Inflammatory Activity: BSA Denaturation Assay - AG-CuONPs nanoparticle was assessed using the BSA denaturation method, with slight modifications (21). 100µL of various concentrations of AG-CuONPs (10, 20, 30, 40, 50 µg/mL), and standard (diclofenac sodium), mixed with 1 mL of 1% w/v BSA prepared in phosphate buffer saline (PBS, pH 6.4), left for 15 to 20 min incubated at 37ºC, then the samples were shifted to water bath for 20 minutes at 60ºC. After getting to room temperature, control was maintained with PBS. Absorbance was recorded at 660 nm. The formula below in equation [2] was used to calculate the % inhibition of BSA denaturation.

$$\text{Inhibition of BSA denaturation (\%)} = \left(\frac{Abs\ of\ Control - Abs\ of\ Sample}{Abs\ of\ Control}\right) \times 100 \qquad [2]$$

Where, Abs = Absorbance or Optical Density (O.D.); control = with PBS; sample = on addition of AG-CuONPS or diclofenac

Egg Albumin Denaturation Assay - In this method, egg albumin (EA) solution (1%, 200µL) was mixed with PBS solution (2.8 mL, 1x, pH 6.4), to which 2 mL of AG-CuONPs (10, 20, 30, 40, 50 µg/mL) and drug diclofenac sodium (standard) were added. This reaction was incubated for 15minutes at room temperature, shifted to a water bath at 60°C to induce denaturation for 20 minutes (21, 22). The absorbance was taken at 660 nm. The inhibition of EA denaturation was determined using the above formula.

Antibacterial Activity: The antibacterial activity of AG-CuONPs was assessed against strains of *P. aeruginosa*, *E. coli*, and *S. aureus*, respectively, in terms of zone of inhibition (23). 200µL of the 0.5 McFarland inoculum was spread over the Mueller-Hinton agar plate. Wells (8 mm diameter) were created using a sterilized 1 mL micropipette tip and filled with 0.1 mL of 25, 50, and 100µg/mL concentrations of AG-CuONPs. The plates were incubated up to 24 hours at 37°C, and the clear zone was measured using an antibiotic zone reader. The common antibiotic Amoxicillin (25 µg) was used to compare the antibacterial activity of bacterial strains.

Cytoplasmic Leakage Analysis: The bacteria colonies were cultured in Nutrient Broth overnight in centrifuge tubes (24). Then treated with different concentrations (10, 20, 30, 40, 50 µg/mL) of Amoxicillin (Positive control) and Ag-CuONPs, for 24 h. The negative control was maintained with Normal saline. The supernatant was collected into an Eppendorf after centrifugation at 3000 RPM for 10 min. 200 µL of supernatant was loaded into a 96-well ELISA plate, and the Optical Density (O.D.) was recorded at 595 nm.

Protein Leakage Assay (Bradford Assay): In a 96-well plate, 25µL of the previously made supernatant and 200µL of Bradford reagent were mixed, followed by incubation at 37°C for 30 – 40 min in the dark, and the absorbance was taken at 595 nm (24). The protein leakage was calculated using equation [3].

$$y = mx + c \qquad [3]$$

Where, y = absorbance; m = slope from standard curve; x = concentration of sample; c = intercept

Antibiofilm Activity: The bacterial culture was incubated at 37°C for 72 h in BHI broth, then this broth was loaded in a 96-well plate, 300 µL per well, incubated for 48 hours with AG-CuONPs (10, 20, 30, 40, 50 µg/mL) along with a positive control (amoxicillin) and one negative control (Methanol). The biofilm formation was observed under the microscope, and the remaining cell debris was removed by washing with 1x PBS. The biofilm fixation was done using 99% methanol, then crystal violet stain (0.1%) for 20 to 30 min (24, 25). Excess stain was rinsed with sterile distilled water for 2-3 times, 250µL of ethanol was added to each well to dissolve bound stain for 20 minutes, and the intensity of colour was recorded at 590 nm using an ELISA microplate reader.

***In Vitro* Anticancer Activity:** Cell Culture - A549 and HEK293 cell lines were cultured in DMEM media (10 parts of FBS and 1 part of antibiotics) in a CO_2 incubator at 37°C with 5% CO_2 supplement. Once cell growth attained 80% confluence, cells were passaged using trypsin and utilised for further experiments.

Cytotoxic Assay (MTT) - A549 and HEK293 monolayers were trypsinized, and 200µL of (10,000 cells/well) cell suspension was loaded to 96-well plates, and allowed to adhere overnight in a CO_2 incubator. The drug treatment was carried out by substituting media with 100 µl of AG-CuONPs (0, 20, 40, 60, 80, 100 µg/mL) in various concentrations that had been prepared in culture media. After 24 hours of drug treatment, to each well, 10µL of MTT reagent was added, and the incubator was set for 4 hours. The formed formazan crystals were dissolved by adding the crystal dissolving (100µL) solution, left for 4 to 18 hours of incubation (26). The absorbance of purple colour was measured using an ELISA reader (imark, Biorad, Japan) at 570 nm. The cell viability was calculated using below equation [4].

$$\text{Cell Viability (\%)} = \left(\frac{Mean\ abs\ of\ treated\ cells}{Mean\ abs\ of\ control\ cells}\right) \times 100 \qquad [4]$$

Where, Abs = Absorbance or Optical density (O.D); Control = without drug treatment; Treated = cells treated with AG-CuONPs

Statistical Analysis

The mean ± SD was calculated to present data. The control and treated cell groups' mean was compared with an unpaired t-test, with more than two individual groups, carried out by ANOVA. The $P \leq 0.05$ (*) was considered significant, significant was cited as asterisk $p \leq 0.001$ (**), $p \leq 0.0001$ (***), and $p < 0.0001$ (****). All statistical analysis were performed using GraphPad Prism (Ver: 10.4.0, San Diego, CA, USA), and the IC_{50} values for cytotoxicity assay were calculated using non-liner regression analysis with dose-response curve-fitting module in GraphPad Prism. All experimentations were done in triplicate (n=3).

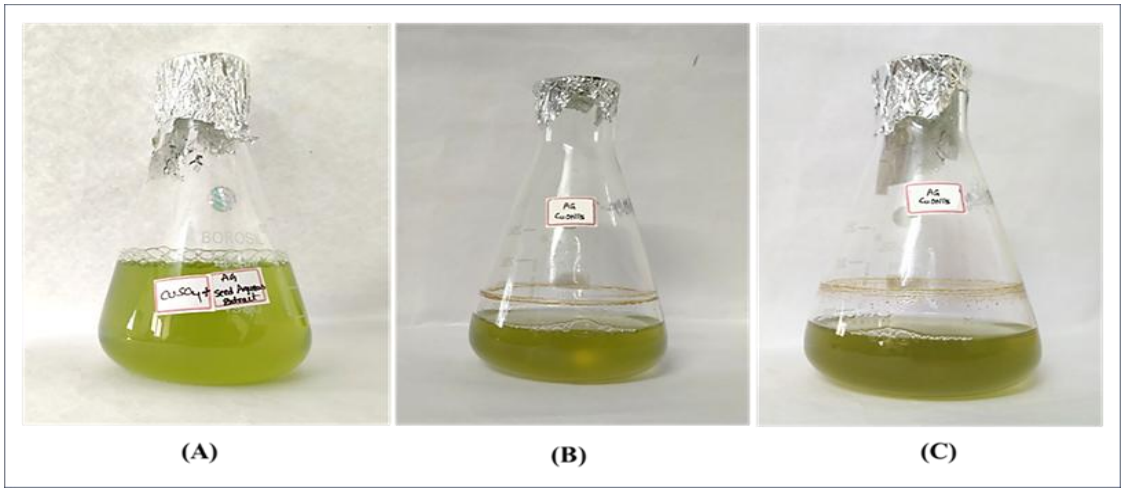

Figure 3: Observational Changes During *A. graveolens* Copper Oxide Nanoparticle Synthesis: A) Initial Colour Change of Copper Sulphate on Addition of *A. graveolens* Extract at 0 hour; B) Colour Changes After 24 hours of Incubation; C) Colour Change from Light Green to Dark Green on 48 hours of Incubation

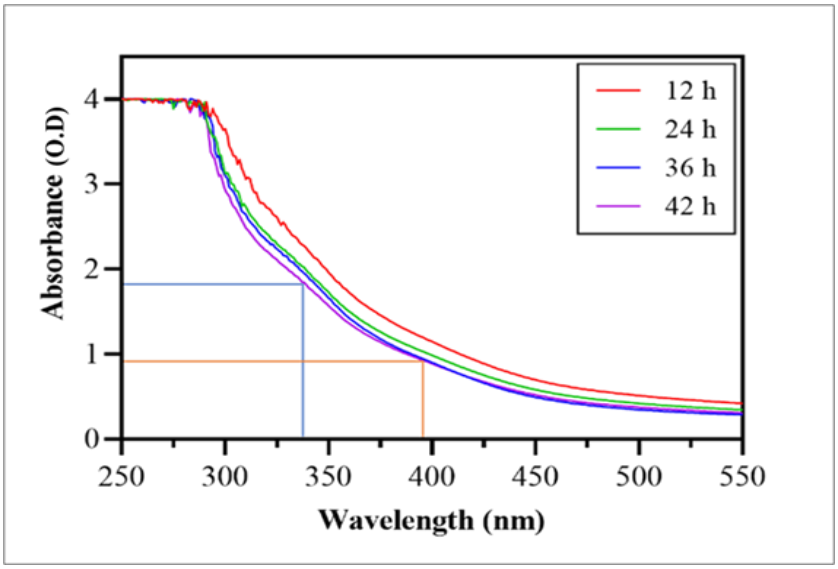

Figure 4. UV-Vis Spectrum of the Synthesized AG-CuONPs at Different Time Points

Results and Discussion

Visual Assessment

On addition of dill seed extract to a 30 mM copper sulphate solution initially turned it yellowish-green from blue (27). During the reaction, from 12 to 48 hours, a deep greenish colour with sediment was observed (Figure 3), indicating the copper oxide nanoparticles formation (27). This was also confirmed by UV-VIS spectrophotometry.

UV–Visible Spectroscopy: The copper oxide nanoparticles exhibited a decrease in absorption (Figure 4) with an increase in reaction time (12, 24, 36, 42 hours), suggesting a progressive reduction in copper ions ($Cu^{2+} \rightarrow Cu^{0}$). This slight shifting and decrease in intensity over time indicate growth and aggregation of nanoparticles, leading to a change in optical properties (28). The broad peaks were observed at 342 and 380 nm, possibly due to polydisperse or slightly aggregated nanoparticles, corresponding to the SPR of Cu-ONPs, confirming the formation of AG-CuONPs (18, 29). The phytochemicals, such as terpenoids, flavonoids, and phenolic compounds, may aid as reducing and stabilizing properties, preventing excessive aggregation (30). The absence of a sharp peak supports the presence of a polydisperse system.

Fourier Transform Infrared Spectroscopy (FTIR): The FTIR spectrum reveals several intense peaks (Figure 5), identifying various functional groups in the synthesis and stabilization process. A broad and highest peak at 3160 cm-^{1} is due to hydroxyl (–OH) groups from phenolic compounds, which were observed to reduce the copper ions. The highest peak at 1632 cm^{-1} corresponds to carbonyl (C=O) or amide (N-H) groups, representing the proteins in the extract. Similar results were observed in previous study, synthesis of copper oxide nanoparticles from *Psidium guajava* leaf extract (31). Further, the peak at 1425 cm^{-1} due to C–H bending vibrations shows the involvement of organic compounds in stabilization, and that at 1224 cm^{-1} represents C–O stretching, and 1073 cm^{-1} indicates C–N stretching vibrations, indicating the involvement of amino groups. Moreover, the peaks at 873 cm^{-1} and 610 cm^{-1} may be due to interactions between functional groups and copper Cu–O bonding. These results were aligned, with research conducted on biosynthesis of CuO-NPs using durian husk extract (32).

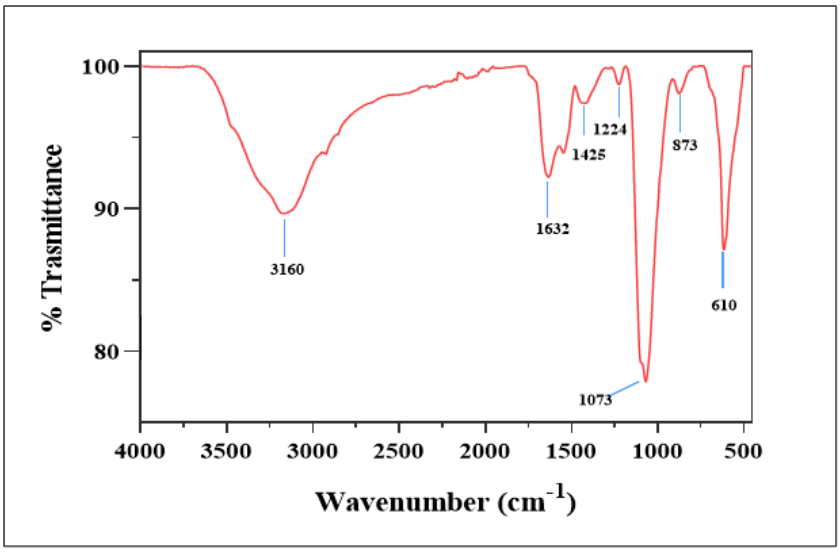

Figure 5: FTIR Spectra of AG-CuONPs

X-ray Diffraction Analysis (XRD): The XRD diffraction pattern showed 23 sharp peaks (Figure 6), confirming partial crystallinity, with the most intense peak at 22.4° (823.85 counts). Major reflections at 24.1°, 31.7°, 32.8°, and 29.2° suggest a face-centered cubic (FCC) copper structure (18, 27). A broad background indicates amorphous organic material from phytochemical capping agents. Quantitative phase analysis revealed 13.4% crystalline and 86.6% amorphous content, suggesting effective reduction and stabilization of CuONPs (27). The crystallite size was calculated by utilizing of Scherrer equation [5].

$$D = \frac{K\lambda}{\beta cos\theta} \qquad [5]$$

Where, D = crystallite size (nm), K is a constant = 0.9, lambda (λ) = 1.54, beta (β) = FWHM, and theta (θ) = Bragg angle in radians (half of 2θ)

The calculated average particle size is 65 ± 23 nm. Similar outcomes have been reported using the chemical liquid deposition method to synthesize CuONPs, while an FCC crystal structure was observed in earlier study on CuNP synthesis utilizing *Hagenia abyssinica* Leaf Extract (33).

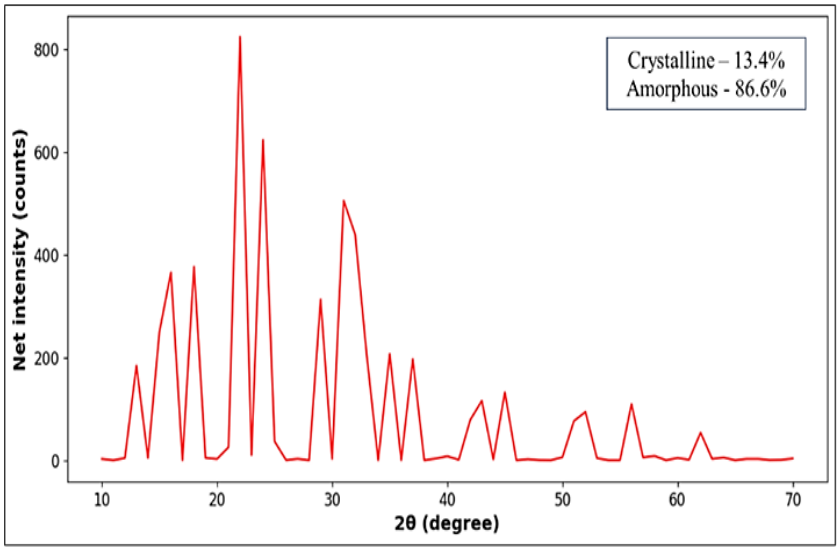

Figure 6: AG-CuONPs XRD Pattern

Morphology Analysis

Scanning Electron Microscope (SEM) with Energy-Dispersive X-ray (EDX): The SEM analysis of AG-CuONPs (Figure 7), characterised by an average particle size range from 40 – 80 nm, is fairly monodispersed, exhibiting predominantly spherical shape, having a relatively smooth surface with agglomeration (34). Elemental analysis by EDX showed a dominant presence of carbon (C) and Oxygen (O), indicating the presence of organic compounds, possibly plant biomolecules, flavonoids, and phenols. Importantly, 0.87% copper (Cu) was detected, confirming the successful synthesis of copper nanoparticles. Additionally, trace elements like Na, Mg, Al, Si, Cl, and Ca were detected, which may originate from the seed extract (18, 35). These high carbon and oxygen levels suggest that phytochemicals of dill extract effectively reduce, cap, and stabilize copper ions. The average size of CuNPs was estimated between 10 – 50 nm, consistent with similar green synthesis studies (27).

Transmission Electron Microscope (TEM): The TEM micrograph (Figure 8) revealed that the AG-CuONPs exhibit irregular, predominantly quasi-spherical to oval shapes that tend to form branched and chain-like aggregates. The particle diameter ranges from 40 to 120 nm, with an average of 45 nm (27). The nanoparticles exhibited smooth and well-defined boundaries, which were supported by the crystalline nature confirmed by XRD analysis. Similar findings were observed in CuNPs synthesised using *Camelia sinensis,* yield particle size range 70 to 80 nm, and an average particle diameter was 60 ± 6nm (35). The observed aggregation into clusters up to ~300 nm suggests the presence of phytochemicals from the extract that aid in stabilization while promoting particle association (18, 36).

Anti-Inflammatory Activity

Concentration-dependent percentages of inhibitory activity were observed with AG-CuONPs and standard in both the BSA denaturation and egg albumin assays (Figure 9). In both assays, the AG-CuONPs demonstrated better anti-inflammatory activity than sodium diclofenac; in the egg albumin assay, half of the protein denaturation inhibition was achieved at 10 µg/mL, whereas in BSA, it is approximately 13.8 µg/mL (37). AG-CuONPs significantly reduced protein denaturation and demonstrated a potent anti-inflammatory effect.

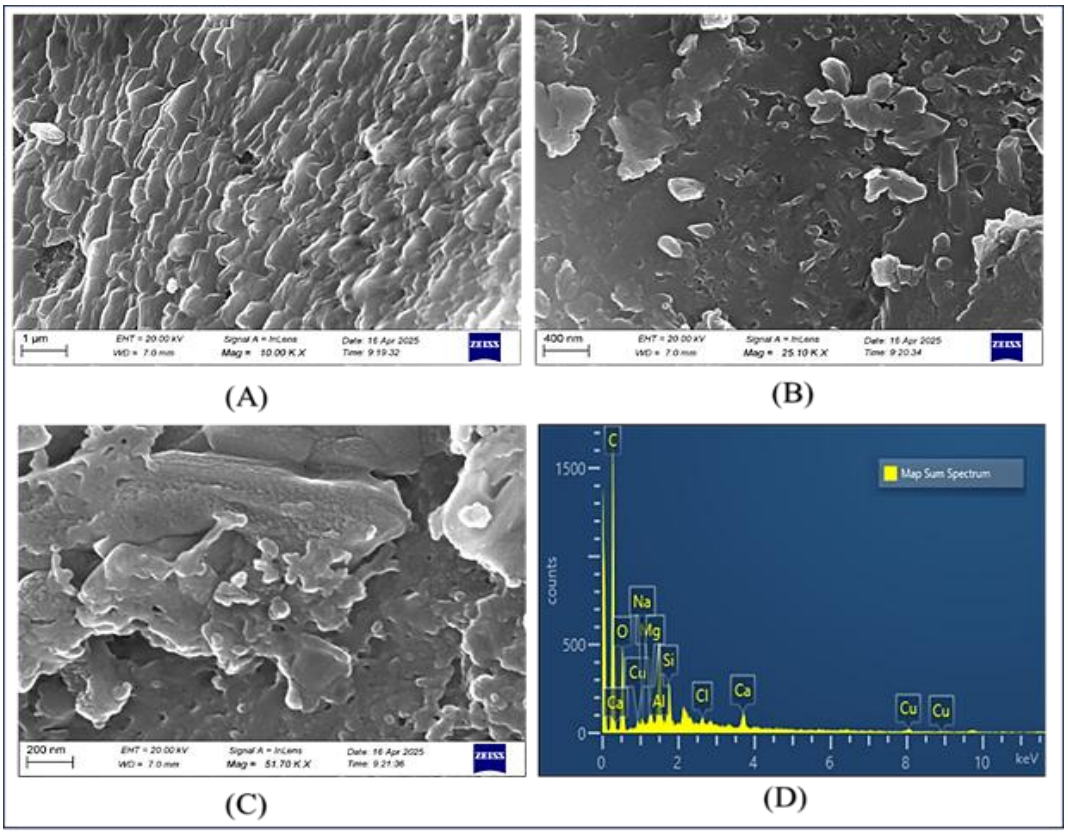

Figure 7: SEM Analysis of AG-CuONPs at Different Magnifications: A) 1µm; B) 400 nm; C) 200 nm; D) EDX

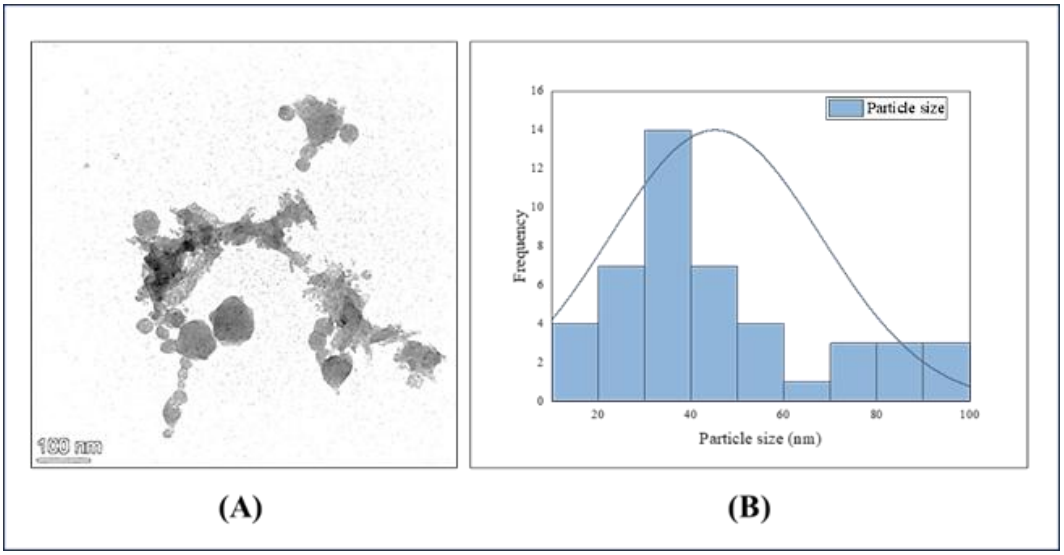

Figure 8: TEM Image of Green-synthesized AG-CuONPs A) Shows Predominantly Spherical Particles with Slight Aggregation at 100 nm Scale, B) Average Particle Size Distribution

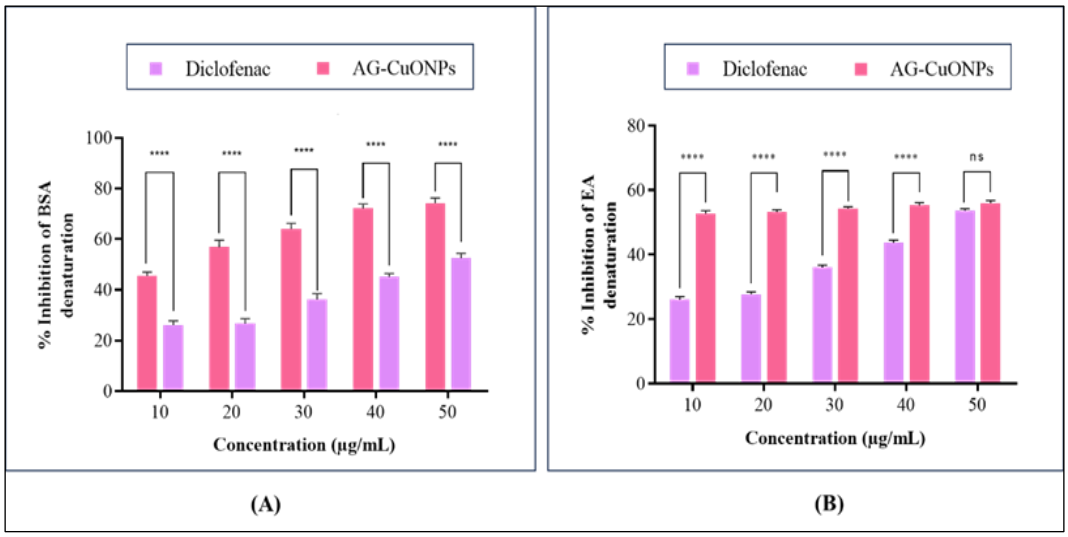

Figure 9: Anti-Inflammatory Activity of AG-CuONPs: A) BSA, B) Egg Albumin (EA)

Bioactive compounds such as chlorogenic acid, linoleic acid, and elaidic acid may reduce the inflammatory response by suppressing the NF-κB pathway by preventing the generation of NO, iNOS, and COX-2 (12). Consequently, inflammatory-promoting cytokines (TNF-α and IL-1β) are expressed at a reduced level. According to the results above, AG-CuONPs exhibit a strong anti-inflammatory effect.

Antioxidant (DPPH): AG-CuONPs exhibited notable free radical scavenging activity, but their antioxidant potential is lower than the standard (Figure 10). The EC_{50} was observed at 11.25 µg/mL for the standard ascorbic acid, while AG-CuONPs had an EC_{50} of 35.06 µg/mL, higher than the standard (38). It shows that a higher concentration is required for 50% inhibition. however, the free radical scavenging activity may be due to the bioactive compounds carveol, perillyl alcohol, limonene, and sabinene (39). A previous study indicated that aqueous dill seed extract presented 50% radical scavenging potential at a lower concentration than ethanolic extract (39, 40), and in another study, silver nanoparticles synthesized from Dill seed extract exhibited Maximum inhibition at 200 to 250µg/ml (41).

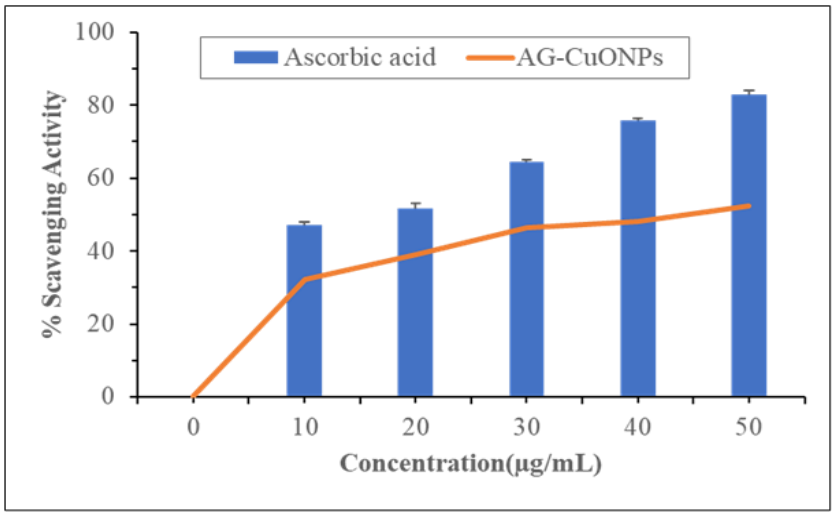

Figure 10: DPPH Radical Scavenging Activity of AG-CuONPs

Antibacterial Activity

AG-CuONPs exhibited concentration-dependent increase in zone of inhibition against all tested bacteria. At concentration of 25µg/mL, the mean zone of inhibition was 7.0 ± 0.44 mm for *S. aureus*, 11.0 ± 0.50 mm for *E. coli* and 16.13 ± 0.81 mm for *P. aeruginosa*, with increase in concentration at 50 µg/mL inhibition was increased to 8.97 ± 0.38, 13.0 ± 0.20, and 20.5 ± 0.70 mm. Maximum activity was observed at 100 µg/mL, with zone of inhibition 11.8 ± 0.65, 17.1 ± 0.47 and 29.9 ± 0.78 mm respectively. The standard drug showed inhibition zones of 19.0 ± 0.79, 28.8 ± 0.76, and 17.0 ± 0.80 mm. Overall results, *S. aureus* demonstrated extensive variance across all AG-CuONPs concentrations, indicating reliable antibacterial effects (Figure 11, 12). The *P. aeruginosa* exhibited great antibacterial activity, followed by *E. coli,* and the lowest activity against *S. aureus* (28, 42). The antimicrobial mechanism of copper nanoparticles was well documented (9). Reactive oxygen species produced by CuONPs can cause oxidative stress, which can damage bacterial cell proteins. Additionally, copper ions released from the nanoparticle can interact with the cell membrane, causing structural disruption, increasing membrane permeability, and ultimately, cell lysis (27, 43). These findings suggest that green-synthesized AG-CuONPs have effective antimicrobial activity, offering a promising alternative to conventional antibiotics.

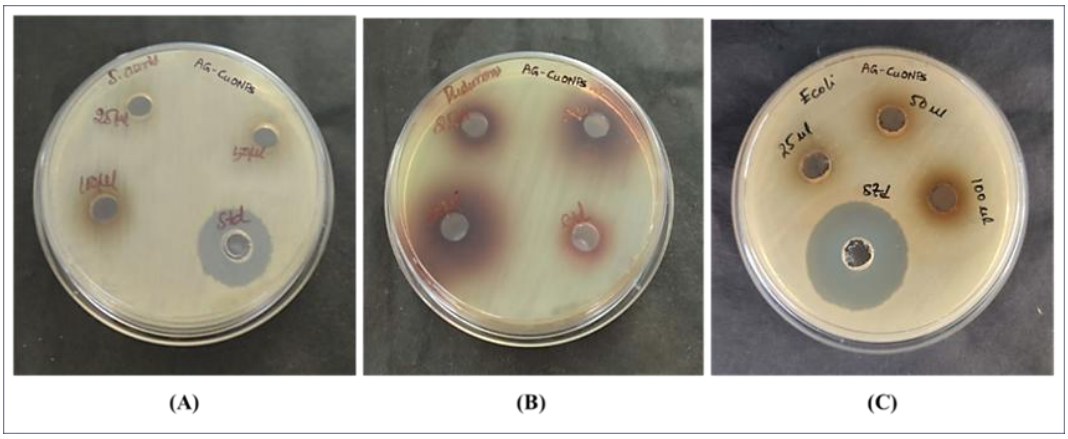

Figure 11: Antibacterial Activity of AG-CuONPs with Amoxicillin Standard (Std). (A) *S. aureus*; (B) *P. aeruginosa*; (C) *E. coli*

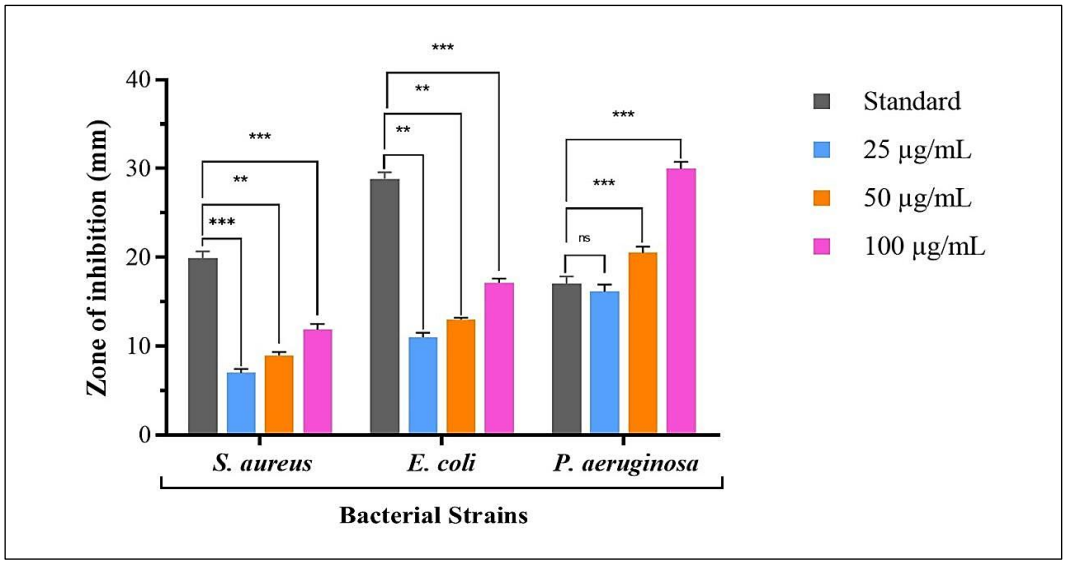

Figure 12: Comparison of Antibacterial Effects between AG-CuONPs and Standard, with Zones of Inhibition (mm)

Cytoplasmic Leakage Assay: The cytoplasmic leakage analysis showed a dose-dependent increase in absorbance in both treated groups with AG-CuONPs and Amoxicillin (Figure 13). The increase in absorbance for all tested bacterial strains, indicating enhanced cytoplasmic leakage. For amoxicillin absorbance at minimal concentration were approximately for *S. aureus* is 0.08 – 0.09, for *E. coli* 0.09 – 0.10, and *P. aeruginosa* 0.11 – 0.12. with increase in concentration, the absorbance was gradually increased, reaching approximately 0.19 – 0.20 in *S. aureus*, 0.20 – 0.21 in *E. coli*, and 0.32 – 0.34 in *P. aeruginosa* at highest concentration. On treatment with AG-CuONPS markedly higher increase in absorbance across all concentrations. Baseline values for *S. aureus*, *E. coli*, and *P. aeruginosa* were 0.115, 0.125, 0.242, which increased substantially with concentration reaching 0.30 – 0.70, 0.57 – 0.70, and 1.32 – 1.39 at higher concentration. Interestingly, *P. aeruginosa* had the most cytoplasmic leakage, followed by *E. coli* and *S. aureus*. When compared with standard (amoxicillin), AG-CuONPs produced more cytoplasmic leakage (44). It could be explained by their multi-target mechanism, which compromises membrane integrity by interacting with the bacterial membrane, producing ROS, and releasing metal ions into the bacterial cell (9, 16, 45). Overall findings show that produced nanoparticles have strong antibacterial action through membrane.

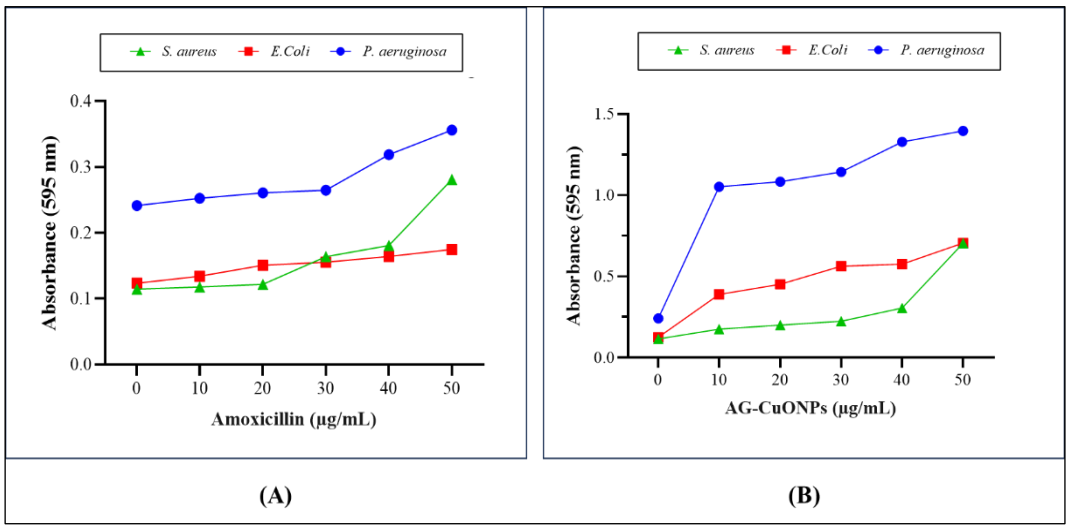

Figure 13: Cytoplasmic Leakage Assay; (A) Amoxicillin, (B) AG-CuONPs

Protein Leakage Assay: Protein leakage increased with concentration of standard drug and AG-CuONPs in all test strains (Figure 14). For the amoxicillin at 10 µg/mL, protein leakage increased to 66.8 in *E. coli*, 63.5 in *S. aureus*, and 77.0 in *P. aeruginosa*. At highest concentration of 50 µg/mL protein leakage was 75.3, 76.7, and 93.0 µg/mL among tested organisms *P. aeruginosa* exhibited consistently higher protein leakage. On treatment with AG-CuONPs at minimal concentration (10µg/mL), protein leakage was 155 µg/mL in *E. coli*, 107 µg/mL in *S. aureus*, and 222 µg/mL in *P. aeruginosa*, indicating early membrane damage. Further increase in concentration resulting progressive elevation of protein leakage. At higher concentration 30 – 50 µg/mL, protein leakage was reached to 192 – 224 µg/mL in *E. coli*, 117 – 250 µg/mL in *S. aureus*, and 291 – 436 µg/mL in *P. aeruginosa*. Maximum leakage was observed with AG-CuONPs compared to amoxicillin in all concentrations. *P. aeruginosa* demonstrated the greatest vulnerability, followed by *S. aureus and E. coli*. According to these results, AG-CuONPs exhibit improved antibacterial potential by protein leakage through disrupting the cell membrane, leading to the malfunction of bacteria, which leads to death (9, 46).

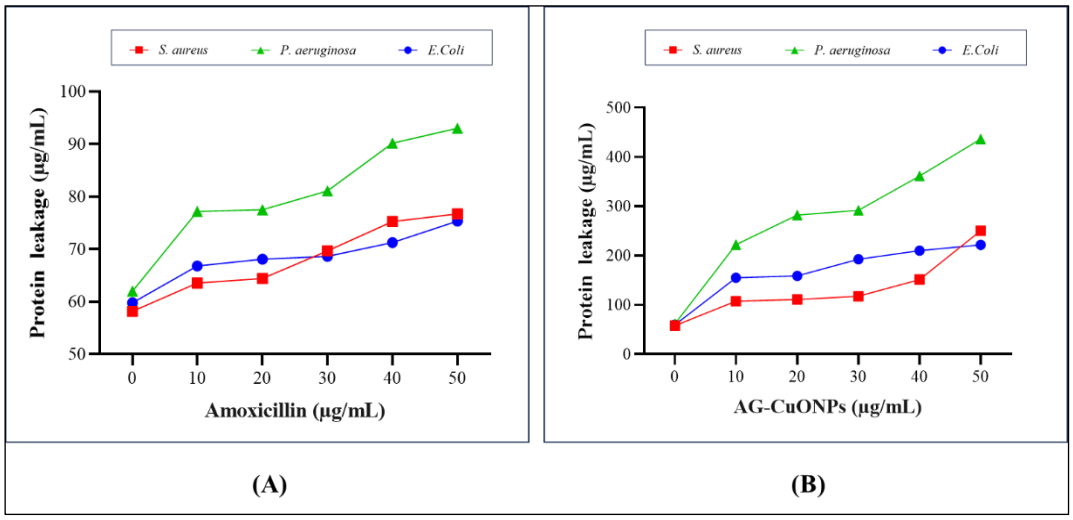

Figure 14: Bradford's Protein Leakage Analysis by both Amoxicillin and AG-CuONPs

Antibiofilm Activity

All three bacterial strains showed a clear dose-dependent increase in antibiofilm activity, progressive decrease in absorbance with increase in treatment concentration indicates reduction in biofilm mass (Figure 15). High absorbance was observed in control, noticeable decline in absorbance was notes at 10µg/mL concentration for *S. aureus* 0.75, 0.59, *P. aeruginosa*, and 0.58 for *E. coli*. With further increase in concertation from 20 – 30 µg/mL absorbance values declined to approximately 0.47 – 0.36 for *S. aureus*, 0.53 – 0.50 for *P. aeruginosa* and 0.50 – 0.45 for *E. coli*. A pronounced reduction was observed at higher concentration, absorbance values reached lowest approximately 0.16 for *S. aureus*, 0.12 for *P. aeruginosa*, and 0.33 for *E. coli* at 50 µg/mL. *S. aureus* and *P. aeruginosa* were the most susceptible strains among all those examined, whereas *E. coli* showed moderate activity, indicating greater susceptibility of *S. aureus* and *P. aeruginosa* (16). These results suggest that the AG-CuONPs effectively inhibit biofilm formation, particularly at higher concentrations. It may be due to the precipitation of proteins in bacteria, by rupture of the cell membrane, through the limonene bioactive compound of *A. graveolens*, which was more effective against biofilm formation (13, 47).

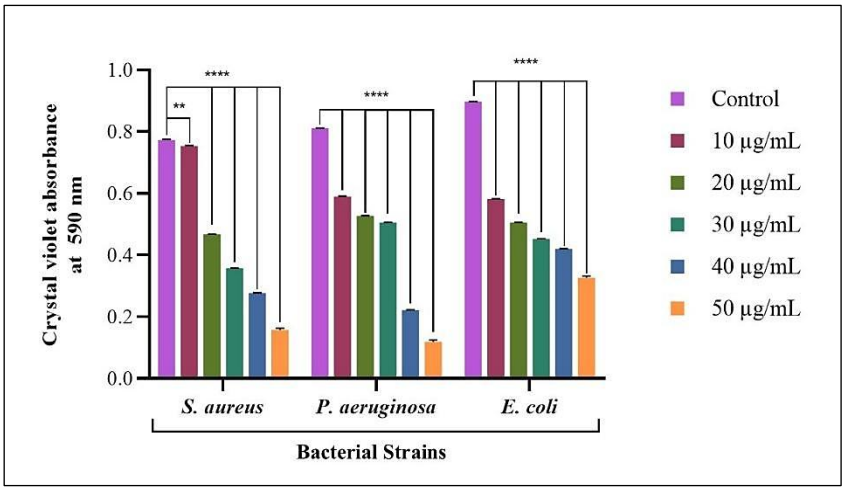

Figure 15: Antibiofilm Activity of AG-CuONPs

Anticancer Activity

Cell viability was reduced in both A549 and HEK293 cell lines in a dose-dependent manner by the biosynthesized AG-CuONPs (Figure 16). In HEK293 cells, viability declined markedly from 87% at 20µg/mL to 60% at 100µmL. however, A549 cells exhibited relatively more response, with viability decreased from 85% at 20µg/mL to 40% at 100µg/mL. Significant differences were found between the cell lines ($p < 0.001$). The IC50 in A549 cells was (68.7 ± 2 µg/mL) and in HEK293 (137.2 ± 2 µg/mL), which was lower in the A549 cell line. According to these findings, AG-CuONPs exhibited more cytotoxicity towards the A549 cell type compared to the normal HEK293. A previous study conducted using the ethyl acetate fraction of *A. graveolens L* in the hepatocarcinoma cell line (HepG2) had shown antiproliferative activity (16, 48). Another study using the *A. graveolens* ethanolic extract showed significant, dose-dependent cytotoxicity against cell lines A549, MCF-7, and HeLa, with the most pronounced effect on MCF-7 breast carcinoma cells. The extract caused oxidative stress, initiated ROS production, lowered mitochondrial membrane potential (MMP), and activated caspase-3 and caspase-9, suggesting apoptosis through the intrinsic pathway, possibly through oxidative stress and mitochondrial dysfunction (40).

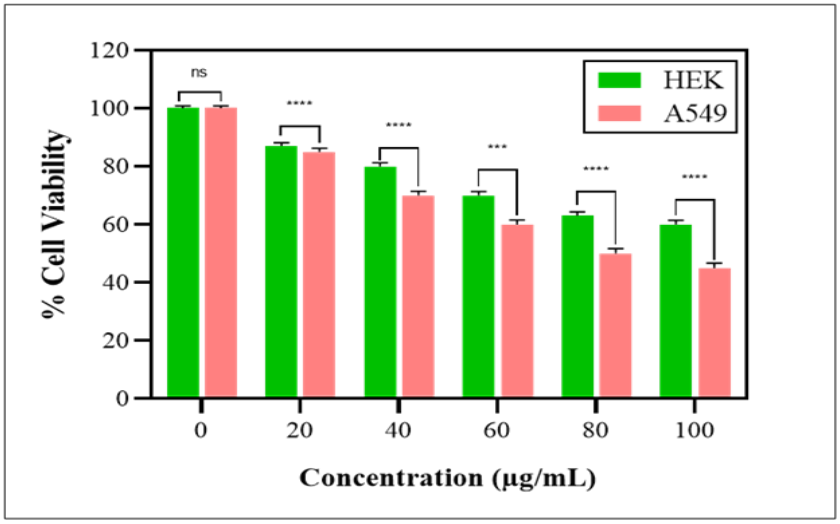

Figure 16: Cytotoxicity Assessment by MTT Assay Followed by Exposure to Various Concentrations of AG-CuONPs

Conclusion

The green synthesized copper oxide nanoparticles (AG-CuONPs) from *A. graveolens* seed extract showed a distinct spherical shape with an average diameter of around 45 nm. AG-CuONPs exhibited dose-dependent antibacterial, antibiofilm, antioxidant, anti-inflammatory, and anticancer activity, protein leakage, and biofilm inhibition, and showed greater anti-inflammatory efficacy. Also, shown greater cytotoxicity to A549 cancer cells, minimal in HEK293 normal cells. These observations demonstrate the multifaceted potential in therapeutic applications, suggest their potential integration in antimicrobial therapies, wound care formulation, anticancer applications, additionally it may suitable for incorporation in to biomedical surface coatings and pharmaceutical delivery system. To improve their translational and clinical usability, more research on dose standardization and formulation optimization is necessary. However more studies were required to study the toxicity profiling, comprising hemocompatibility, long-term toxicity, and its molecular mechanism in anticancer activity, including regulatory pathways involved, necessary prior to application in clinical practice.

Limitations

Novelty of this study lies in linking green synthesis of CuONPs using *A. graveolens* with enhanced biological performance. Nevertheless, the investigations are limited to in-*vitro* assessment, and detailed mechanism and molecular pathways were not fully explored. Future research should be prioritizing *in vivo* validation, molecular-level studies, and improve specificity and safety.

Abbreviations

AG-CuONPs: *Anethum graveolens* mediated Copper Oxide Nanoparticles, DPPH: 2,2-diphenyl-1-picrylhydrazyl, IC50: Half Maximum Inhibitory Concentration, MTT: 3- (4,5-dimethylthiazol-2-yl)-2,5-diphenyltetrazolium bromide.

Acknowledgement

The authors thanks Meenakshi Academy of Higher Education and Research for invaluable support.

Author Contributions

Kodiganti Naresh Kumar: performed the experiments, collected the data, drafted the manuscript, Tharani Munusamy: supervised the study, provided technical guidance, Malchi Suresh: performed the experiments, collected the data, drafted the manuscript, Manju Bhargavi S: performed the statistical analysis, Nalini Devarajan: conceptualization, methodology, review, editing. All authors interpreted the results and critically reviewed and revised the final manuscript.

Conflict of Interest

The authors declare that there is no conflict of interest regarding the publication of this article.

Declaration of Artificial Intelligence (AI) Assistance

Open AI was used to make frame work of manuscript, summarizing content and Grammarly was used to check grammar.

Ethical Approval

There were no human and animal participants in this study; therefore, ethical approval was not applicable.

Funding

In this research, no funds were received from any organization.

References

1. Osanloo M, Ghanbariasad A, Taghinezhad A. Antioxidant and anticancer activities of *Anethum graveolens* L., *Citrus limon* (L.) *Osbeck* and *Zingiber officinale Roscoe* essential oils. Trad Integr Med 2021;6(4):333-347.
2. Kurul F, Turkmen H, Cetin AE, Topkaya SN. Nanomedicine: How nanomaterials are transforming drug delivery, bio-imaging, and diagnosis. Next Nanotechnology. 2025;7(100129):100129.
3. Jadoun S, Arif R, Jangid NK, Meena RK. Green synthesis of nanoparticles using plant extracts: a review. Environ Chem Lett. 2021;19(1):355–74.
4. El-Meligy MA, Abd El-Monaem EM, Eltaweil AS, Mohy-Eldin MS, Ziora ZM, Heydari A, Omer AM. Recent advancements in metallic Au-and Ag-based chitosan nanocomposite derivatives for enhanced anticancer drug delivery. Molecules. 2024;29(10):2393.
5. Karahmet Sher E, Alebić M, Marković Boras M, *et al*. Nanotechnology in medicine revolutionizing drug delivery for cancer and viral infection treatments. Int J Pharm. 2024;660(124345):124345.
6. Hernández-Guadarrama A, López-Ayuso CA, Garza-Hernández R, *et al*. Eco-friendly synthesis of copper oxide nanoparticles using geranium Pelargonium x hortorum leaf extract and its biological applications. Pharmaceutics. 2025;17(12):1562
7. Pohanka M. Copper and copper nanoparticles toxicity and their impact on basic functions in the body. Bratisl Lek Listy. 2019;120(6):397–409.

8. Pandey MM, Rastogi S, Rawat AKS. Indian traditional ayurvedic system of medicine and nutritional supplementation. Evid Based Complement Alternat Med. 2013;2013:376327.
9. Ivanova IA, Daskalova DS, Yordanova LP, Pavlova EL. Copper and copper nanoparticles applications and their role against infections: A minireview. Processes (Basel).2024;12(2):352.
10. Antonio-Pérez A, Durán-Armenta LF, Pérez-Loredo MG, Torres-Huerta AL. Biosynthesis of copper nanoparticles with medicinal plants extracts: From extraction methods to applications. Micromachines (Basel). 2023;14(10):1882.
11. Datiles,Marianne Jennifer, Acevedo-Rodriguez, Pedro. cabicompendium.3472, CABI Compendium, CABI, *Anethum graveolens* (dill); 2015. https://www.cabidigitallibrary.org/doi/10.1079/cabicompendium.3472
12. Nam H-H, Nan L, Choo B-K. Anti-inflammation and protective effects of *Anethum graveolens* L. (dill seeds) on esophageal mucosa damages in reflux esophagitis-induced rats. Foods. 2021;10(10):2500.
13. Noumi E, Ahmad I, Adnan M, *et al*. GC/MS profiling, antibacterial, anti-quorum sensing, and antibiofilm properties of *Anethum graveolens* L. essential oil: Molecular docking study and in-silico ADME profiling. Plants. 2023;12(10):1997.
14. Yadav G, Sonigra P, Meena M. A review on pharmaceutical and medicinal importance of *Anethum graveolens* L. Acta Sci. Nutr. Health. 2022;6(7):23-8.
15. Mohammed FA, Elkady AI, Syed FQ, Mirza MB, Hakeem KR, Alkarim S. *Anethum graveolens* (dill) – A medicinal herb induces apoptosis and cell cycle arrest in HepG2 cell line. J Ethnopharmacol.2018;219:15–22.
16. Mashraqi A. Induction role of chitosan nanoparticles to *Anethum graveolens* extract against food-borne bacteria, oxidant, and diabetic activities in *vitro*. Front Microbiol.2023;14:1209524.
17. Hadi N, Drioiche A, Bouchra EM, *et al*. Phytochemical analysis and evaluation of antioxidant and antimicrobial properties of essential oils and seed extracts of *Anethum graveolens* from southern Morocco: In *vitro* and in silico approach for a natural alternative to synthetic preservatives. Pharmaceuticals (Basel). 2024;17(7):862.
18. Ghosh MK, Sahu S, Gupta I, Ghorai TK. Green synthesis of copper nanoparticles from an extract of *Jatropha curcas* leaves: characterization, optical properties, CT-DNA binding and photocatalytic activity. RSC Adv. 2020;10(37):22027–35.
19. Dhanraj G, Rajeshkumar S. Anticariogenic effect of selenium nanoparticles synthesized using *Brassica oleracea*. J Nanomater. 2021; 2021:1–9.
20. Tharani M, Rajeshkumar S, Al-Ghanim KA, Nicoletti M, Sachivkina N, Govindarajan M. *Terminalia chebula*-assisted silver nanoparticles: Biological potential, synthesis, characterization, and ecotoxicity. Biomedicines. 2023;11(5):1472.
21. Rajakumari R, Volova T, Oluwafemi OS, Rajeshkumar S, Thomas S, Kalarikkal N. Nano formulated proanthocyanidins as an effective wound healing component. Mater Sci Eng C Mater Biol Appl. 2020;106(110056):110056.
22. Ameena M, Arumugham M, Ramalingam K,Rajeshkumar S. Evaluation of the anti-inflammatory, antimicrobial, antioxidant, and cytotoxic effects of chitosan thiocolchicoside-lauric acid nanogel. Cureus.2023;15(9): e46003.
23. Kaur GJ, Arora DS. Antibacterial and phytochemical screening of *Anethum graveolens*, *Foeniculum vulgare* and *Trachyspermum ammi*. BMC Complement Altern Med. 2009;9(1):30.
24. Munusamy T, Shanmugam R. Green synthesis of copper oxide nanoparticles synthesized by *Terminalia chebula* dried fruit extract: Characterization and antibacterial action. Cureus. 2023;15(12):e50142.
25. Swidan NS, Hashem YA, Elkhatib WF, Yassien MA. Antibiofilm activity of green synthesized silver nanoparticles against biofilm associated enterococcal urinary pathogens. Sci Rep. 2022;12(1):3869.
26. Karthik C, Pillai RR, Moreno GH, Sikder P, Ambalavanan N, Thomas V. Plasma/ozone induced PolyNaSS graft-polymerization onto PEEK biomaterial for bio-integrated orthopedic implants. JOM (1989). 2024;76(10):5662–74.
27. Murthy HA, Desalegn T, Kassa M, Abebe B, Assefa T. Synthesis of green copper nanoparticles using medicinal plant *Hagenia abyssinica* (Brace) JF. Gmel. leaf extract: Antimicrobial properties. J Nanomater. 2020;2020(1):3924081.
28. Rajeshkumar S, Menon S, Kumar V, Ponnanikajamideen M, Ali D, Arunachalam K. Anti-inflammatory and antimicrobial potential of *Cissus quadrangularis*-assisted copper oxide nanoparticles. J Nanomater. 2021; 2021:1–11.
29. Vishveshvar K, Aravind Krishnan MV, Haribabu K, Vishnuprasad S. Green synthesis of copper oxide nanoparticles using *ixiro coccinea* plant leaves and its characterization. Bionanoscience. 2018;8(2):554–8.
30. Jadhav VK, Pawar SS. Qualitative and quantitative analysis of *Anethum graveolens* L. leaves in various extracts. Adv. Zool. Bot. 2023;11(5):392-8.
31. Relhan A, Guleria S, Bhasin A, Mirza A, Zhou JL. Biosynthesized copper oxide nanoparticles by *Psidium guajava* plants with antibacterial, antidiabetic, antioxidant, and photocatalytic capacity. Biomass Convers Biorefin. 2025;15(19):26623–40.
32. Liang YP, Chan YB, Aminuzzaman M, *et al.* Green synthesis and characterization of copper oxide nanoparticles from durian (*Durio zibethinus*) husk for environmental applications. Catalysts. 2025;15(3): 275.
33. Eslami A, Modanlou Juibari N, Hosseini SG, Abbasi M. Synthesis and characterization of CuO nanoparticles by the chemical liquid deposition method and investigation of its catalytic effect on the thermal decomposition of ammonium perchlorate. Cent Eur J Energetic Mater. 2017;14(1):152–68.
34. Belurkar R. Synthesis and characterization of Lanthanum nanoparticles by *Anethum Graveolens* (dill) leaf extract. Orient J Chem. 2021;37(5):1205–9.
35. Ahmed A, Usman M, Liu Q-Y, Shen Y-Q, Yu B, Cong H-L. Plant mediated synthesis of copper nanoparticles by using *Camelia sinensis* leaves extract and their applications in dye degradation. Ferroelectrics. 2019;549(1):61–9.
36. Qiu Y, Mu Z, Wang N, Wang X, Xu M, Li H. The aggregation and sedimentation of two different sized copper oxide nanoparticles in soil solutions: Dependence on pH and dissolved organic matter. Sci Total Environ. 2020;731(139215):139215.

37. Kazemi M. Phenolic profile, antioxidant capacity and anti-inflammatory activity of *Anethum graveolens* L. essential oil. Nat Prod Res. 2015;29(6):551–3.
38. Kaur GJ, Arora DS. Antibacterial and phytochemical screening of *Anethum graveolens*, *Foeniculum vulgare* and *Trachyspermum ammi*. BMC Complement Altern Med. 2009;9(1):30.
39. Shyu YS, Lin JT, Chang YT, Chiang CJ, Yang DJ. Evaluation of antioxidant ability of ethanolic extract from dill (*Anethum graveolens* L.) flower. Food Chem. 2009;115(2):515-21.
40. Al-Oqail MM, Farshori NN. Antioxidant and anticancer efficacies of *Anethum graveolens* against human breast carcinoma cells through oxidative stress and caspase dependency. BioMed Research International. 2021;2021(1):5535570.
41. Zare-Bidaki M, Mohammadparast-Tabas P, Khorasha-dizade M, *et al*. Bio-synthesized AGS@AgNPs for wound healing, antioxidant support, antibacterial defense, and anticancer intervention. Biocatal Agric Biotechnol. 2024; 61:103402.
42. Derakhshan S, Navidinia M, Ahmadi A. Antibacterial activity of Dill (*Anethum graveolens*) essential oil and antibiofilm activity of Cumin (*Cuminum cyminum*) alcoholic extract. Infect. epidemiol. microbiol. 2017;3(4):122-6.
43. Vijayakumar G, Kesavan H, Kannan A, Arulanandam D, Kim JH, Kim KJ, Song HJ, Kim HJ, Rangarajulu SK. Phytosynthesis of copper nanoparticles using extracts of spices and their antibacterial properties. Processes. 2021;9(8):1341.
44. Asghar MA, Asghar MA. Green synthesized and characterized copper nanoparticles using various new plants extracts aggravate microbial cell membrane damage after interaction with lipopolysaccharide. Int J Biol Macromol. 2020; 160:1168–76.
45. Okoye UC, Okhamafe AO, Arhewoh MI. Biosynthesis of copper oxide nanoparticles and evaluation of their antimicrobial properties. Int J Pharm Pharm Sci. 2023; 15(5): 8-15.
46. Ahmed RS, Dahham AM, Abdalameer NK, Mohammed RS. Reduction of silver oxide nanoparticles using *Anethum graveolens* leaves extract and assessment of their antibacterial and antibiofilm properties. Research Square. 2024. https://doi.org/10.21203/rs.3.rs-4689900/v1
47. Popa M, Măruțescu L, Oprea E, *et al*. In *vitro* evaluation of the antimicrobial and immunomodulatory activity of culinary herb essential oils as potential perioceutics. Antibiotics (Basel). 2020;9(7):428.
48. El-Zehery HRA, Ashry NM, Faiesal AA, Attia MS, Abdel-Maksoud MA, El-Tayeb MA, Aufy M, El-Dougdoug NK. Antibacterial and anticancer potential of bioactive compounds and secondary metabolites of endophytic fungi isolated from *Anethum graveolens*. Front Microbiol.2024;15:1448191.

How to Cite: Kumar KN, Munusamy T, Suresh M, Bhargavi SM, Devarajan N. Biogenic Synthesis of Copper Oxide Nanoparticles using *Anethum graveolens*; Antibacterial, Anticancer and Therapeutic Potential in vitro Analysis. Int Res J Multidiscip Scope. 2026; 7(1): 799-814. DOI: 10.47857/irjms.2026.v07i01.07489